NJC

PAPER

View Article Online
View Journal

Cite this: DOI: 10.1039/c6nj00692b

Synthesis, structural characterization, electrochemical behavior and anticancer activity of gold(III) complexes of *meso*-1,2-di(1-naphthyl)-1,2-diaminoethane and tetraphenylporphyrin†

Muhammad Altaf,[a] Saeed Ahmad,[b] Abdel-Nasser Kawde,[c] Nadeem Baig,[c] Abdullah Alawad,[d] Saleh Altuwaijri,[e] Helen Stoeckli-Evans[f] and Anvarhusein A. Isab*[c]

Received (in Montpellier, France) 3rd March 2016,
Accepted 1st August 2016

DOI: 10.1039/c6nj00692b

www.rsc.org/njc

Three gold(III) complexes, $[Au(npen)Cl_2]Cl{\cdot}2H_2O$ (**1**), $[Au(npen)_2]Cl_3$ (**2**) and [Au(TPP)]Cl (**3**) (npen = *meso*-1,2-di(1-naphthyl)-1,2-diaminoethane, TPP = *meso*-tetraphenylporphyrin) have been synthesized and characterized using elemental analysis, IR and NMR spectroscopy, and one of them (**1**) by X-ray crystallography. The structure of **1** consists of a $[Au(npen)Cl_2]$ complex ion, a chloride counter ion and two water molecules. The gold atom in the complex ion adopts a distorted square planar geometry. The interactions of **1** and **2** with L-tyrosine, glutathione and lysozyme were studied electrochemically. The electrochemical measurements indicated that gold(III) remained stable and did not undergo reduction upon interaction with proteins. The *in vitro* cytotoxic properties of the complexes as well as of cisplatin were evaluated on three human cancer cell lines, A549 (lung cancer cells), MCF7 (breast cancer cells) and HCT15 (colon cancer cells) using MTT assay. The results indicated that the prepared gold(III) complexes were more potent than cisplatin in inhibiting the growth of the selected cancer cells. The IC_{50} data revealed that complex **3** was the most effective antiproliferative agent.

1. Introduction

Today gold(III) complexes constitute an important class of potential anticancer agents because of their strong cytotoxic effects against selected human cancer cell lines.[1–10] However, their low stability under physiological conditions remains a critical parameter in the drug development of these species because of their high reduction potential and fast hydrolysis rate.[10–13] These problems can possibly be circumvented by forming gold(III) compounds with one or more multidentate nitrogen-donor ligands to enhance their stability.[1–6,9,11,15] In this regard, during the past two decades, promising antitumor gold(III) complexes containing nitrogen-donor polyaromatic ligands, such as terpyridine and phenanthroline derivatives, have been prepared and tested for their antitumor activity.[10–21] Messori *et al.* reported the solution chemistry and the cytotoxic properties of several mono- and di-nuclear complexes, which include $[Au(en)_2]Cl_3$, $[Au(phen)Cl_2]Cl$, $[Au_2(phen^{2Me})_2(\mu\text{-}O)_2](PF_6)_2$, $[Au(bipy)(OH)_2][PF_6]$, $[Au_2(2,2'\text{-bipyridine})_2(\mu\text{-}O)_2][PF_6]_2$, $[Au(dien)_2Cl]Cl_2$, $[Au(terpy)Cl]Cl_2$ and $[Au(cyclam)](ClO_4)_2Cl$.[10–15] The coordination of polyamine ligands caused a marked stabilization of gold in the +3 oxidation state as indicated by measurements of the reduction potentials. With the exception of the cylam species, $[Au(cyclam)](ClO_4)_2Cl$, all complexes displayed good cytotoxic effects against different cancer cells.[11,15] Gold(III) complexes of quinoline and its derivatives were also found to demonstrate significant tumor inhibition due to the formation of stable chelates. Some of them were even more active than cisplatin.[16,17]

Recently, we have evaluated the antiproliferative properties of some gold(III)-diamine complexes, particularly of 1,2-diaminocyclohexane, and the results illustrate that they possess promising anticancer activities against a number of cells.[18–24] Similarly, the *in vitro* cytotoxic evaluation of gold(III) complexes with esters of cyclohexyl-functionalized ethylenediamine-*N*,*N*′-diacetate

[a] Center of Excellence in Nanotechnology (CENT), King Fahd University of Petroleum and Minerals, Dhahran 31261, Saudi Arabia
[b] Department of Chemistry, College of Sciences and Humanities, Prince Sattam bin Abdulaziz University, Al-Kharj 11942, Saudi Arabia
[c] Department of Chemistry, King Fahd University of Petroleum and Minerals, Dhahran 31261, Saudi Arabia. E-mail: aisab@kfupm.edu.sa
[d] National Center for Stem Cell Technology (NCSCT), Life Sciences and Environmental Research Institute, King Abdulaziz City for Science and Technology (KACST), Riyadh 11442, Saudi Arabia
[e] Clinical Research Laboratory, SAAD Research Development Center, SAAD Specialist Hospital, Al-Khobar 31952, Saudi Arabia
[f] Institute of Physics, University of Neuchâtel, rue Emile-Argand 11, CH-2000 Neuchâtel, Switzerland

† CCDC 1447950. For crystallographic data in CIF or other electronic format see DOI: 10.1039/c6nj00692b

or -dipropanoate showed that their cytotoxic action was comparable to that of cisplatin.[25,26] Gold(III)-dithiocarbamates have also received considerable attention as potential anticancer agents because of their strong cell growth-inhibitory effects.[27–29]

Gold(III) porphyrins might be regarded as a novel class of cytotoxic agents for nasopharyngeal carcinoma (NPC) and hepatocellular carcinoma (HCC) cells.[3,30–32] They were found to be stable in DMSO, as well as under physiologically-relevant conditions.[3] The gold(III)-porphyrin complex, [Au(TPP)]Cl (H2TPP = tetraphenylporphyrin), exhibited potent *in vitro* anticancer activities towards a panel of cancer cell lines, including cisplatin- and multi-drug resistant cell lines.[33] Its toxicity to the cancer cells was ~10 fold higher than to the normal cells, and thus it opened a safe therapeutic window for anti-NPC treatment.[3] Moreover, *in vivo* and *in vitro* binding assays indicated that it interacted with the DNA in a non-covalent manner, which was different from cisplatin.[34]

Based on the structural and electronic similarity of gold(III) complexes to cisplatin and related platinum antitumor drugs, it was expected that their activity was due to binding with DNA. But several studies indicate that DNA is not the main biological target of the gold(III) complexes since most of them are found to have weak binding affinity to DNA.[5,8,10,13,34,35] Gold(III) complexes on the other hand have shown high reactivity towards different protein models and inhibition of a few crucial proteins seems to be the main mechanism of action for cytotoxic gold complexes.[5,10,36,37] Particularly, in some studies proteasomes have been identified as the major *in vitro* and *in vivo* target for gold(III) complexes.[38,39] Moreover, these compounds are able to activate mitochondrial death pathways, since they markedly inhibit the activity of mitochondrial selenoenzyme, thioredoxin reductase.[26,40]

Inspired by the promising results of our previous studies,[18–24] we are deeply interested in further investigating the structural features and antitumor effects of gold(III)-diamine complexes. Consequently, we report here the synthesis, structural characterization and electrochemical and antiproliferative evaluation of two new gold(III) complexes (**1** and **2**) of a diamine, *meso*-1,2-di(1-naphthyl)-1,2-diaminoethane (npen). The antitumor properties of the tetraphenylporphyrin (TPP) complex (**3**) are also reported, which previously have been evaluated for other types of cancer cells.[30–34] The interactions of **1** and **2** with model proteins were also studied by cyclic voltammetry.

2. Experimental

2.1. Chemicals

Sodium tetrachloridoaurate(III) dihydrate ($NaAuCl_4 \cdot 2H_2O$), *meso*-1,2-di(1-naphthyl)-1,2-diaminoethane (npen) and tetraphenylporphyrin (TPP) were purchased from Sigma-Aldrich Chemical Co. L-Tyrosine, lysozyme, L-glutathione, ethanol, sodium dihydrogen phosphate, and disodium hydrogen phosphate were purchased from Sigma-Aldrich (USA). Double distilled water was used for electrochemical measurements and was obtained from a Lab based Water Still Aquatron A 4000 D unit. 3-(4,5-Dimethylthiazol-2-yl)-2,5-diphenyltetrazolium bromide, a yellow tetrazole, was purchased from Sigma Chemical Co, St. Louis, MO, USA.

2.2. Synthesis of complexes

Compounds **1**, $[Au(npen)Cl_2]Cl \cdot 2H_2O$ and **2**, $[Au(npen)_2]Cl_3$ were prepared by mixing 200 mg (0.5 mmol) of $NaAuCl_4 \cdot 2H_2O$ and 157 mg (0.5 mmol) or 315 mg (1 mmol) of *meso*-1,2-di(1-naphthyl)-1,2-diaminoethane (npen) for **1** and **2**, respectively, in 20 mL water and stirring the mixture continuously for 1 hour. The resulting orange (for **1**) or yellow (for **2**) precipitates were collected by filtration. The products were dried in air at room temperature. Yield: 86% (280.88 mg) for **1** and 79% (366.87 mg) for **2**. Suitable crystals of complex **1** were obtained as small golden-yellow rods by slow evaporation of its methanol/water solution.

Complex **3**, [Au(TPP)]Cl, was prepared by the reported procedure.[31,33] Yield: 72% (305.17 mg).

The elemental analysis of the complexes is given in Table 1.

2.3. IR and NMR measurements

The IR spectra of the ligands and their gold(III) complexes were recorded on a Perkin-Elmer FT-IR 180 spectrophotometer using KBr pellets over the range 4000–400 cm^{-1}. All NMR measurements were carried out on a Jeol JNM-LA 500 NMR spectrophotometer at 297 K. The ^1H NMR spectra were recorded at a frequency of 500.00 MHz. The ^{13}C NMR spectra were obtained at a frequency of 125.65 MHz with ^1H broadband decoupling and referenced relative to TMS. The spectral conditions were: 32k data points, 0.967 s acquisition time, 1.00 s pulse delay and 45 degrees pulse angle.

2.4. Spectroscopic data

IR (KBr pellet, cm^{-1}): npen, ν = 3384, 3317, 3051, 2900, 1594, 1507, 1386, 1260, 1139, 1075, 994; **1**, ν = 3446, 2916, 2852, 1647, 1513, 1403, 1268, 774; **2**, ν = 3414, 3040, 2924, 2857, 1514, 776; TPP, ν = 3449, 3300, 3053, 1596, 1440, 1347, 1069, 1002, 967, 793, 726, 695; **3**, ν = 3440, 3304, 3045, 1585, 1399, 1002, 967, 726.

^1H NMR (500 MHz, DMSO, 24 °C, TMS, ppm): npen, δ = 1.84, 5.08, 7.26, 7.33, 7.40, 7.50, 7.71, 7.84, 7.86; **1**, δ = 1.21, 5.89, 7.24, 7.34, 7.40, 7.54, 7.95, 7.97, 10.40; **2**, δ = 5.45, 7.1–9.1 (multiplet); TPP, δ = 7.81, 8.11, 8.20, 8.84; **3**, 7.19, 7.82, 8.25, 8.84.

^{13}C NMR (125.65 MHz, DMSO, TMS, ppm): npen, δ = 50.60, 123.27, 124.52, 125.18, 126.85, 128.45, 131.73, 133.06, 139.59, 177.89; **1**, δ = 51.86, 125.04, 125.87, 126.11, 126.63, 127.95, 128.77, 129.73, 130.50, 178.53; **2**, 52.28, 122.25, 124.82, 125.55, 126.04, 128.50, 130.96, 132.43, 132.71, 178.65.

Table 1 Elemental analysis and melting points of gold(III) complexes

	Found (calculated) %		
Compound	C	H	N
1	39.98 (40.54)	3.81 (3.71)	4.25 (4.30)
2	57.15 (56.94)	4.28 (4.34)	5.97 (6.04)
3	62.77 (62.53)	3.25 (3.34)	6.53 (6.63)

2.5. X-ray structure determination

The intensity data of **1** were collected at 203 K (−70 °C) on a Stoe Mark II-Image Plate Diffraction System[41] equipped with a two-circle goniometer and using MoKα graphite monochromated radiation (λ = 0.71073 Å). The structure was solved by direct methods using SHELX-97.[42] The refinement and all further calculations were carried out using SHELX-2014.[43] All the H atoms could be located in difference Fourier maps.

In the final cycles of refinement, the water H atoms were refined with distance restraints (O–H = 0.84(2) Å and H···H = 1.35(2) Å) with U_{iso}(H) = 1.5U_{eq}(O). The NH_2 and C-bound H atoms were included in the calculated positions and treated as riding atoms: N–H = 0.90 Å and C–H = 0.94–0.99 Å with U_{iso}(H) = 1.2U_{eq}(C). The non-H atoms were refined anisotropically, using weighted full-matrix least-squares on F^2. A semi-empirical (multi-scan) absorption correction was applied using the MULABS routine in PLATON.[44] The figures were drawn using the program, Mercury.[45] A summary of crystal data and refinement details for compound **1** is given in Table 2.

2.6. *In vitro* cytotoxic activity of complexes

To examine the possible anticancer effect of complexes (**1–3**) and cisplatin, a panel of three human tumor cell lines, A549 (lung cancer cells), MCF7 (breast cancer cells) and HCT15 (colon cancer cells) was used. The different human carcinoma cell cultures (A549, MCF7, HCT15) were first seeded at the concentration of 2×10^4 cells per mL in their respective growth media containing 10% FBS (fetal bovine serum) in a 96-well tissue culture plate and were incubated for 72 h at 37 °C, 5% CO_2 in air and 90% relative humidity in a CO_2 incubator. After that the cell cultures were incubated for 24 h with 100 μL of cisplatin and the complexes (**1–3**) having 100, 50, 25 and 12.5 μM concentrations, prepared in the growth medium. Furthermore, the cultures were incubated with 100 μL of vital mitochondrial tetrazolium dye (3-(4,5-dimethylthiazol-2-yl)-2,5-diphenyltetrazolium bromide) (0.5 mg ml^{-1}) in a CO_2 incubator at 37 °C in the dark for 4 h. After incubation, purple colored formazan crystals were formed due to the reduction of the dye by the mitochondrial succinate dehydrogenase enzyme. The resultant crystals were solublized by adding 100 μL of dimethylsulfoxide (DMSO). The colored solution formed was thoroughly mixed and read spectrophotometrically at 570 nm using a Lab systems Multiskan EX-Enzyme-linked immunosorbent assay (EX-ELISA) reader against a reagent blank. All data presented are mean ± standard deviation.

Table 2 Crystal data and structure refinement details of compound **1**

CCDC deposit no.	1447950
Chemical formula	$C_{22}H_{20}AuCl_2N_2^+ \cdot Cl^- \cdot 2(H_2O)$
Molecular weight	651.75
Crystal system, space group	Triclinic, $P\bar{1}$
Temperature (K)	203
a, b, c (Å)	9.1800 (6), 9.4741 (6), 14.4358 (10)
A, β, γ (°)	90.556 (6), 107.977 (5), 97.243 (5)
V (Å^3)	1183.12 (14)
Z	2
μ (mm^{-1})	6.58
Crystal size (mm)	0.20 × 0.10 × 0.10
T_{min}, T_{max}	0.773, 1.000
No. of measured, independent and observed [$I > 2\sigma(I)$] reflections	13 452, 4761, 4057
R_{int}	0.070
$(\sin\theta/\lambda)_{max}$ (Å^{-1})	0.621
$R[F^2 > 2\sigma(F^2)]$, w$R(F^2)$, S	0.039, 0.091, 0.99
No. of restraints	—
No. of parameters	283
Largest diff. peak and hole (e Å^{-3})	1.59, −2.55
$\Delta\rho_{max}$, $\Delta\rho_{min}$ (e Å^{-3})	

2.7. Protein interaction studies by electrochemical measurements

The voltammetric measurements were performed by using three electrode based Auto Lab electrochemical workstation (Netherland). The working electrode was a glassy carbon electrode (GCE), while Ag/AgCl and platinum were used as reference counter electrodes, respectively. The weights of the chemicals were measured by using a GR-2000 electrical balance. The pH of the buffer was controlled using an Accumet® XL50 pH meter. For electrochemical analysis, compounds **1** and **2** were dissolved in ethanol as their solubility was very poor in aqueous medium. Prior to each analysis, the GCE was polished to a mirror like surface with alumina slurry on the synthetic cloth. The cyclic voltammograms for various analyses were recorded from 0.0 V to +1.3 V with a scan rate of 0.1 V s^{-1}.

3. Results and discussion

3.1. Spectroscopic characterization

The IR spectrum of npen showed the N–H, C–H, and C–N absorption stretching bands at 3384 and 3317, 3053 and 2900, and 1002 cm^{-1} respectively. The N–H bending vibration was observed at 1594 cm^{-1}. These bands also appeared in the spectra of **1** and **2** suggesting the formation of these complexes. The IR spectrum of TPP is characterized by the N–H, C–H, C═N and C═C stretching vibrations, which were observed at 3300, 3053, 1596, and 1468 and 1440 cm^{-1} respectively. Broad peaks around 3440 cm^{-1} represent the O–H groups. The aromatic C–H bending vibrations were observed around 700 cm^{-1}. The presence of these bands in the spectrum of complex **3** indicates the coordination of TPP to the metal center.

The NMR data of the ligands and complexes is listed in Section 2.4. In the ^{1}H NMR spectrum of npen, the CH_2 and N–H resonances were observed at 1.84 and 5.08 ppm, respectively. For aromatic protons, the expected seven signals were observed between 7 and 8 ppm. In the spectrum of **1** these resonances were also clear but in the case of **2** a bunch of peaks was observed in the region of 7.5–9.1 ppm. The ^{1}H NMR spectra of TPP and its complex showed four signals associated with aromatic protons. In the ^{13}C NMR spectra of npen and its complexes (**1** and **2**) the CH_2 resonance of npen was observed around 51 ppm. Nine signals were observed for the aromatic carbon atoms of npen; the one at 128 ppm being more intense represents two carbon atoms. The C-1 atom of naphthyl attached to diamino ethane appeared at the most downfield position.

Upon coordination, the resonances were shifted slightly downfield. The downfield shift is attributed to the shift of electron density from the ligand towards the metal.

3.2. X-ray structure description

The molecular crystal structure of complex **1** is shown in Fig. 1. The selected bond distances and angles are given in Table 3. Compound **1** is mononuclear and consists of a complex cation, $[Au(npen)Cl_2]^+$, a chloride counter ion and two water molecules of crystallization. The central gold(III) ion in **1** is coordinated by two nitrogen atoms of the *meso*-1,2-di-1-naphthyl-ethylenediamine (npen) ligand and two chloride ions. It adopts a somewhat distorted square planar geometry as indicated by the bond angles around the gold center (Table 3). The N–Au–N *cis* angle of 83.8(2) is less than 90° owing to the strain of the diamine ligand after coordination. The *trans* angles (175.11(2)°) are close to linear geometry. These values are in agreement with the values of other gold(III)-diamine complexes.[19–24,46,47] The Au–N bond distances in **1** are almost equal (2.034(5) and 2.029(6) Å), and resemble to those in [Au{*cis*/*trans*-(±)-1,2-DACH}Cl_2]Cl.[19] However, they are somewhat different from the Au–N distances in $[Au(en)Cl_2]Cl{\cdot}2H_2O$,[46] $[Au(en)Cl_2]NO_3$[47] and [Au{1*R*,2*R*-(−)-1,2-DACH}Cl_2]Cl·0.5H_2O.[24] The Au–Cl bond distances of 2.272(2) and 2.274(2) Å are very close to the reported values of the related structures.[19,20,24,46,47] The complex cation and chloride ions are associated with each other through electrostatic and H-bonding interactions. All the chloride ions, both amine groups and water molecules are engaged in hydrogen bonding with each other. The complex molecules pack head to head to generate molecular chains along the *a* and *c* axes (Fig. 2). The N–H···Cl hydrogen bonding interactions involving the Cl^- anion result in the formation of a dimer as shown in Fig. 3.

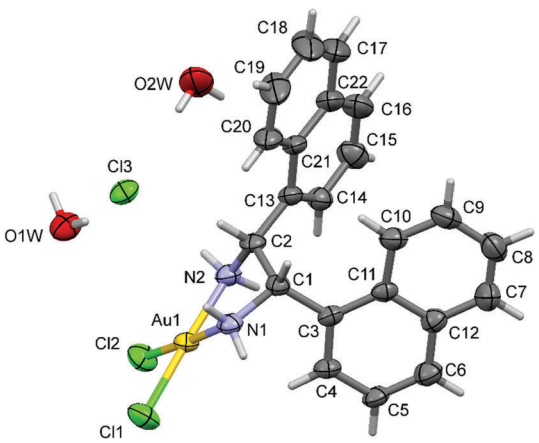

Fig. 1 The molecular structure of **1** along with the atomic numbering scheme. The displacement ellipsoids are drawn at the 50% probability level.

Table 3 Selected bond distances (Å) and bond angles (°) for **1**

Bond distances		Bond angles	
Au(1)–N(1)	2.034(5)	N(1)–Au(1)–N(2)	83.8(2)
Au(1)–N(2)	2.029(6)	N(1)–Au(1)–Cl(1)	91.29(2)
Au(1)–Cl(1)	2.272(2)	N(1)–Au(1)–Cl(2)	175.11(2)
Au(1)–Cl(2)	2.274(2)	N(2)–Au(1)–Cl(1)	175.11(2)
		N(2)–Au(1)–Cl(2)	91.34(2)
		Cl(1)–Au(1)–Cl(2)	93.54(7)

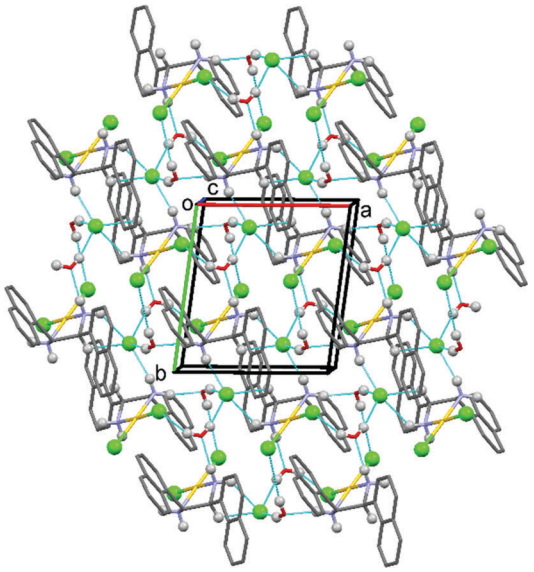

Fig. 2 The crystal packing of the complex **1**, viewed along the *c* axis, illustrating the formation of the hydrogen bonded two-dimensional network parallel to the *ab* plane.

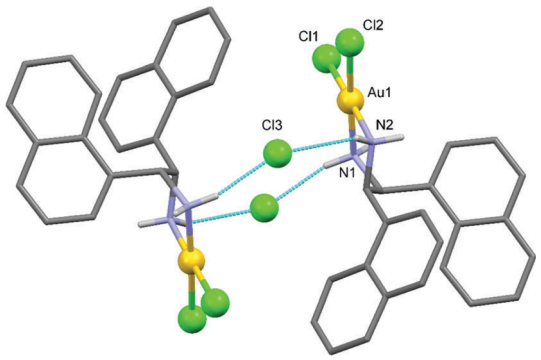

Fig. 3 A view of the formation of the dimer of **1** formed by N–H···Cl hydrogen bonds involving the Cl^- anion.

3.3. Anticancer activity

The anticancer activity of complexes **1–3** as well as cisplatin was evaluated against a panel of representative human tumor cell lines, which include, lung cancer cells (A549), breast cancer cells (MCF7) and colon cancer cells (HCT15). The results of *in vitro* cytotoxic activity are expressed as IC_{50} (concentration causing 50% reduction in cell viability) and are presented in Table 4. It can be seen that the investigated complexes displayed significantly greater cytotoxicity than cisplatin in all three cell lines (Table 4). Among the complexes, **3** exhibited the strongest antiproliferative potency, while **1** is the least active. For **1**, the IC_{50} values are closer to cisplatin. On going from **1** to **2**, the substitution of two chlorine atoms by the chelating diamine ligand brought about a 1.5–3 times decrease in the

Table 4 IC_{50} values (in μM) of gold(III) complexes for different cell lines

Sample	IC_{50}		
	A549	MCF7	HCT15
1	28.76 ± 4.02	11.85 ± 2.60	9.40 ± 1.93
2	10.34 ± 2.82	7.77 ± 1.82	4.23 ± 1.31
3	5.13 ± 1.17	3.36 ± 0.72	3.50 ± 0.73
Cisplatin	42.88 ± 1.99	23.12 ± 3.78	23.12 ± 3.78

antiproliferative activity of **2**. As $[Au\text{-}porphyrin]^+$ is known to be a very effective anticancer agent,[30–33] complex **3** containing a porphyrin ring showed very high activity as compared to cisplatin. It is about 7–8 times more potent than cisplatin against the same cancer cells. It is even more effective against nasopharyngeal carcinoma (NPC) and hepatocellular carcinoma (HCC) cells.[30–32] The IC_{50} values reported here are comparable to those obtained for the gold(III) complexes of 1,2-diaminocyclohexane (DACH) against SGC901 and PC3 cells reported in our previous studies.[19,22,23] It seems that the complexes with such bulky ligands and with a greater degree of chelation may be more effective for the antiproliferative activity.

The survival of the cells (A549, MCF7 and HCT15) was studied by varying the concentration of compounds **1–3**. The percentage of cell viability at various concentrations of gold(III) compounds is shown in Fig. 4. The data obtained represents the concentration-dependent cytotoxic effect against the human cancer cells. As the concentration decreases the cell viability increases. It appears that the gold(III) complexes are better in reducing cell viability than cisplatin.

3.4. Protein interaction studies of complexes 1 and 2

Recently, we have evaluated the electrochemical behavior and the interaction of similar complexes with well-known model proteins.[23,48] To get an insight into the reactivity of the complexes, the interactions of **1** and **2** with model proteins, L-tyrosine, glutathione and lysozyme were studied electrochemically. The electrochemical behavior of compounds **1** and **2** in the presence of proteins was analyzed by a cyclic voltammetric technique (CV). As shown in Fig. 5, two CV irreversible anodic peaks appeared at +0.973 V and +0.982 V for **1** and **2**, respectively. The highly electroactive amino acid L-tyrosine[49] was selected to demonstrate the degree of interaction of these anticancer compounds with amino acids. As a control experiment, the CV response of 0.1 mM complex **1**, as shown in Fig. 5A(b), retained the same peak current intensity and peak shape even after spiking the same volume of the solvent blank used to prepare the L-tyrosine solution in the interaction study.

The sequential spiking of L-tyrosine into a cell containing 0.1 mM compound **1** has shown a significant effect on the peak of the complex. At lower concentration levels of L-tyrosine, the peak of the complex decreased, and almost disappeared at around 320 μM of L-tyrosine (Fig. 5A(e)). A sharp peak of 320 μM L-tyrosine appeared at 0.654 V in the absence of the gold compounds (Fig. 5A(d) and B(d)). However, that peak was shifted to +0.712 V in the presence of **1** and its current significantly decreased (Fig. 5A(e)), which could be attributed to the interaction

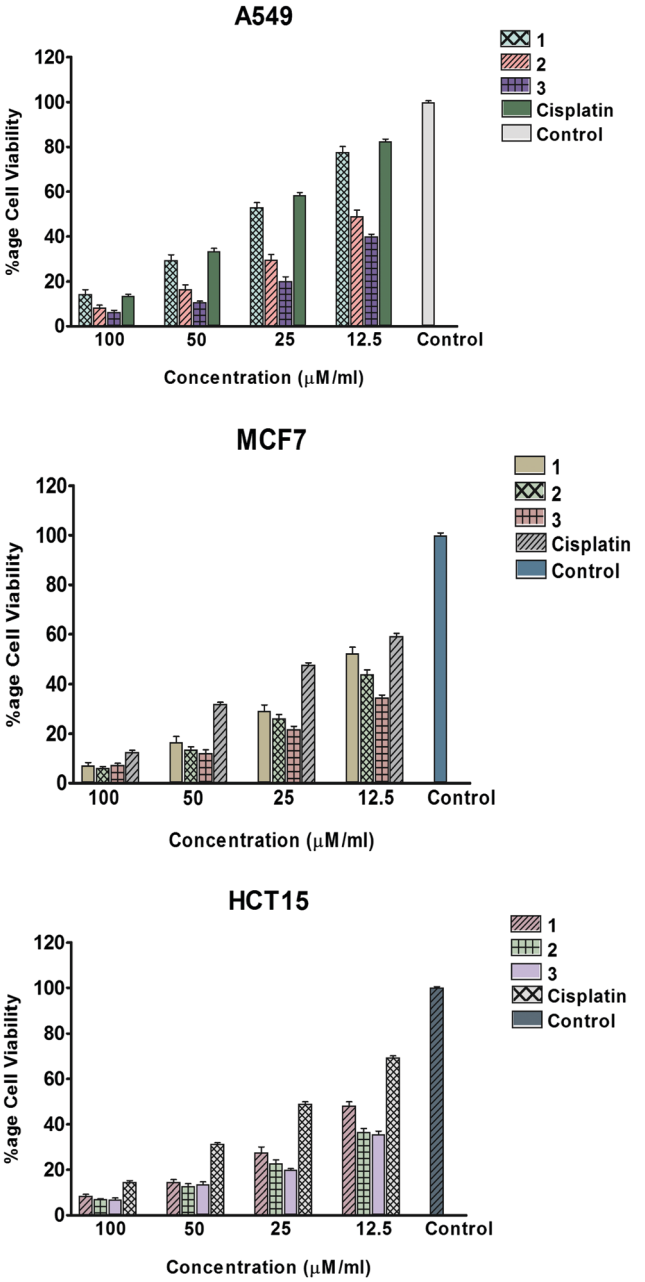

Fig. 4 The survival of the cells as a function of concentration of the complexes.

taking place between the drug and the L-tyrosine. Similar behavior was observed for complex **2** (Fig. 5B(d)) with a reduced peak shift of +0.672 V observed compared to **1** (Fig. 5B(e)). Thus, complex **1** is concluded to have more interaction with L-tyrosine.

The interaction of the compounds was also investigated with glutathione, which is a crucial antioxidant in animals. An interaction was observed for both compounds (**1**, **2**) with glutathione. The first spike of 20 μM of glutathione into 0.1 mM **1** or **2** caused a negative peak shift of the complexes to +0.942 and +0.955 V, respectively (Fig. 6). Subsequent spikes of glutathione into the electrochemical cell containing the 0.1 mM of **1** and **2** showed a systematic decrease in the

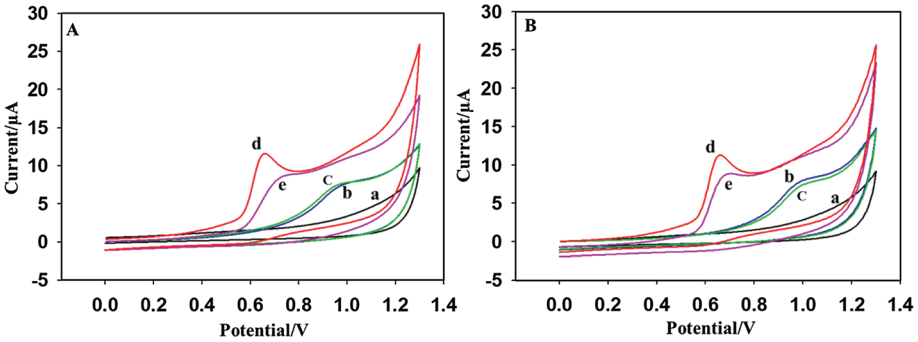

Fig. 5 Cyclic voltammograms in 0.1 M phosphate buffer solution (pH 7.0) of compounds **1** (A) and **2** (B): (a) blank, (b) 0.1 mM complex, (c) addition of 192 μL of L-tyrosine solution solvent blank, and 320 μM L-tyrosine in the absence (d), and presence (e) of the 320 μM L–0.1 mM complex at the GCE. The cyclic voltammograms were recorded at 0.1 V s^{-1} scan rate, and 120 s adsorption time.

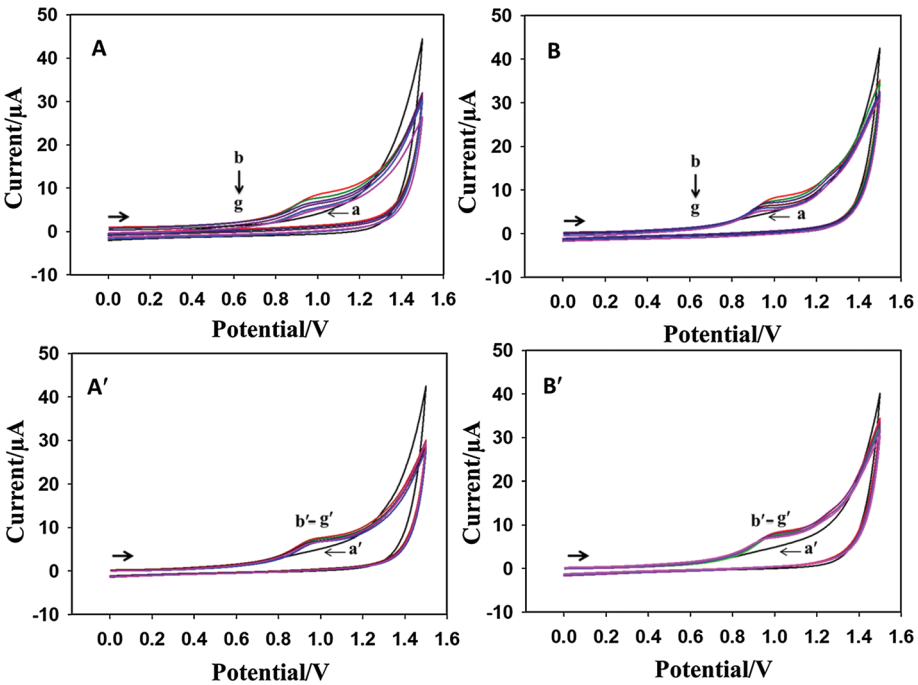

Fig. 6 Cyclic voltammograms of compounds **1** (A) and **2** (B) and corresponding control experiment (A′ and B′) in 0.1 M phosphate buffer solution (pH 7.0). (a, a′) Blank, 0.1 mM MR57 (A) or MR58 (B) in the presence of glutathione at different concentrations: (b, b′) 0 μM, (c) 20 μM, (d) 40 μM, (e) 60 μM, (f) 80 μM and (g) 100 μM. The response of glutathione solution solvent blank (c′) 12 μL, (d′) 24 μL, (e′) 36 μL, (f′) 48 μL and (g′) 60 μL.

registered peak currents of both complexes (Fig. 6A and B). In a control experiment (Fig. 6A′ and B′), both compounds retained the same peak current.

Moreover, the interaction of these compounds was also explored with the lysozyme protein attained from chicken egg white. The successive addition of lysozyme into a solution containing 0.2 mM **1** or **2** showed a decrease in the current intensities of the complex peaks. This interaction was more significant for complex **1** compared to that of **2** (data not shown).

4. Conclusion

In this contribution, we reported the synthesis of two new gold(III) complexes and the crystal structure of one of them (**1**). The analytical and spectroscopic data confirm the formation of complexes. The X-ray structure of compound **1** reveals that the gold atom adopts a square planar coordination environment. Complexes **1** and **2** showed strong interaction with L-tyrosine, glutathione, and the lysozyme protein, and the gold(III) center remained stable during the reaction as indicated by cyclic voltammetric measurements. Complex **1** is concluded to have more interaction with L-tyrosine, glutathione and the lysozyme protein than that of complex **2**. The prepared compounds (**1–3**) were tested for *in vitro* antiproliferative activity against three human tumor cell lines. All three complexes exhibited remarkable cytotoxic properties and especially compound **3** showed potential for clinical testing against the studied cancer cells. These findings could be the subject of further pharmacological investigations.

Acknowledgements

This project was funded by the National Plan for Science and Innovation (MARIFAH)–King Abdulaziz City for Science and Technology (KACST) through the Science and Technology Unit at King Fahd University of Petroleum and Minerals (KFUPM) of Saudi Arabia, award No. 14-MED64-04.

References

1 B. Bertrand and A. Casini, *Dalton Trans.*, 2014, **43**, 4209–4219.
2 C. Nardon, G. Boscutti and D. Fregona, *Anticancer Res.*, 2014, **34**, 487–492.
3 S. Medici, M. Peana, V. M. Nurchi, J. L. Lachowicz, G. Crisponi and M. A. Zoroddu, *Coord. Chem. Rev.*, 2015, **284**, 329–350.
4 R. W.-Y. Sun and C.-M. Che, *Coord. Chem. Rev.*, 2009, **253**, 1682–1691.
5 I. Ott, *Coord. Chem. Rev.*, 2009, **253**, 1670–1681.
6 A. Casini, C. Hartinger, C. Gabbiani, E. Mini, P. J. Dyson, B. K. Keppler and L. Messori, *J. Inorg. Biochem.*, 2008, **102**, 564–575.
7 C.-M. Che and R. W.-Y. Sun, *Chem. Commun.*, 2011, **47**, 9554–9560.
8 T. Zou, C. T. Lum, C.-N. Lok, J.-J. Zhang and C.-M. Che, *Chem. Soc. Rev.*, 2015, **44**, 8786–8801.
9 W. Liu and R. Gust, *Chem. Soc. Rev.*, 2013, **42**, 755–773.
10 A. Casini, G. Kelter, C. Gabbiani, M. A. Cinellu, G. Minghetti, D. Fregona, H. H. Fiebig and L. Messori, *J. Biol. Inorg. Chem.*, 2009, **14**, 1139–1149.
11 L. Messori, F. Abbate, G. Marcon, P. Orioli, M. Fontani, E. Mini, T. Mazzei, S. Carotti, T. O. Connell and P. Zanello, *J. Med. Chem.*, 2000, **43**, 3541–3548.
12 M. A. Cinellu, L. Maiore, M. Manassero, A. Casini, M. Arca, H.-H. Fiebig, G. Kelter, E. Michelucci, G. Pieraccini, C. Gabbiani and L. Messori, *ACS Med. Chem. Lett.*, 2010, **1**, 336–339.
13 A. Casini, M. A. Cinellu, G. Minghetti, C. Gabbiani, M. Coronnello, E. Mini and L. Messori, *J. Med. Chem.*, 2006, **49**, 5524–5531.
14 G. Marcon, S. Carotti, M. Coronello, L. Messori, E. Mini, P. Orioli, T. Mazzei, M. A. Cinellu and G. Minghetti, *J. Med. Chem.*, 2002, **45**, 1672–1677.
15 S. Carotti, A. Guerri, T. Mazzei, L. Messori, E. Mini and P. Orioli, *Inorg. Chim. Acta*, 1998, **281**, 90–94.
16 T. Yang, C. Tu, J. Zhang, L. Lin, X. Zhang, Q. Liu, J. Ding, Q. Xu and Z. Guo, *Dalton Trans.*, 2003, 3419–3424.
17 C. Martín-Santos, E. Michelucci, T. Marzo, L. Messori, P. Szumlas, P. J. Bednarski, R. Mas-Balleste, C. Navarro-Ranninger, S. Cabrera and J. Alemán, *J. Inorg. Biochem.*, 2016, **153**, 339–345.
18 A. A. Isab, M. N. Shaikh, M. Monim-ul-Mehboob, B. A. Al-Maythalony, M. I. M. Wazeer and S. Altuwaijri, *Spectrochim. Acta, Part A*, 2011, **79**, 1196–1201.
19 S. S. Al-Jaroudi, M. Fettouhi, M. I. M. Wazeer, A. A. Isab and S. Altuwaijri, *Polyhedron*, 2013, **50**, 434–442.
20 M. Monim-ul-Mehboob, M. Altaf, M. Fettouhi, A. A. Isab, M. I. M. Wazeer, M. N. Shaikh and S. Altuwaijri, *Polyhedron*, 2013, **61**, 225–234.
21 S. S. Al-Jaroudi, M. Monim-ul-Mehboob, M. Altaf, M. Fettouhi, M. I. M. Wazeer, S. Altuwaijri and A. A. Isab, *New J. Chem.*, 2014, **38**, 3199–3211.
22 S. S. Al-Jaroudi, M. Monim-ul-Mehboob, M. Altaf, A. A. Al-Saadi, M. I. M. Wazeer, S. Altuwaijri and A. A. Isab, *BioMetals*, 2014, **27**, 1115–1136.
23 S. S. Al-Jaroudi, M. Altaf, A. Al-Saadi, A.-N. Kawde, S. Altuwaijri, S. Ahmad and A. A. Isab, *BioMetals*, 2015, **28**, 827–844.
24 K. H. Omer, A. A. Seliman, M. Altaf, N. Casagrande, D. Aldinucci, S. Altuwaijri and A. A. Isab, *Polyhedron*, 2015, **102**, 773–781.
25 N. Pantelić, B. B. Zmejkovski, J. Trifunović-Macedoljan, A. Savić, D. Stanković, A. Damjanović, Z. Juranić, G. N. Kaluđerović and T. J. Sabo, *J. Inorg. Biochem.*, 2013, **128**, 146–153.
26 N. Pantelić, T. P. Stanojković, B. B. Zmejkovski, T. J. Sabo and G. N. Kaluđerović, *Eur. J. Med. Chem.*, 2015, **90**, 766–774.
27 L. Cattaruzza, D. Fregona, M. Mongiat, L. Ronconi, A. Fassina, A. Colombatti and D. Aldinucci, *Int. J. Cancer*, 2011, **128**, 206–215.
28 C. Marzano, L. Ronconi, F. Chiara, M. C. Giron, I. Faustinelli, P. Cristofori, A. Trevisan and D. Fregona, *Int. J. Cancer*, 2011, **129**, 487–496.
29 L. Ronconi, L. Giovagnini, C. Marzano, F. Bettìo, R. Graziani, G. Pilloni and D. Fregona, *Inorg. Chem.*, 2005, **44**, 1867–1881.
30 Y. F. To, R. W.-Y. Sun, Y. Chen, V. S.-F. Chan, W.-Y. Yu, P. K.-H. Tam, C.-M. Che and C.-L. S. Lin, *Int. J. Cancer*, 2009, **124**, 1971–1979.
31 C. T. Lum, Z. F. Yang, H. Y. Li, R. W.-Y. Sun, S. T. Fan, R. T. P. Poon, M. C. M. Lin, C.-M. Che and H. F. Kung, *Int. J. Cancer*, 2006, **118**, 1527–1538.
32 C. T. Lum, A. S.-T. Wong, M. C. M. Lin, C.-M. Che and R. W.-Y. Sun, *Chem. Commun.*, 2013, **49**, 4364–4366.
33 C.-M. Che, R. W.-Y. Sun, W.-Y. Yu, C.-B. Ko, N. Zhu and H. Sun, *Chem. Commun.*, 2003, 1718–1719.
34 Y. Wang, Q.-Y. He, R. W.-Y. Sun, C.-M. Che and J.-F. Chiu, *Eur. J. Pharmacol.*, 2007, **554**, 113–122.
35 L. Messori, P. Orioli, C. Tempi and G. Marcon, *Biochem. Biophys. Res. Commun.*, 2001, **281**, 352–360.
36 Y. Wang, Q. Y. He, C. M. Che and J. F. Chiu, *Proteomics*, 2006, **6**, 131–142.
37 B. D. Glišić, U. Rychlewska and M. I. Djuran, *Dalton Trans.*, 2012, **41**, 6887–6901.
38 V. Milacic, D. Chen, L. Ronconi, K. R. L. Piwowar, D. Fregona and Q. P. Dou, *Cancer Res.*, 2006, **66**, 10478–10486.
39 V. Milacic and Q. P. Dou, *Coord. Chem. Rev.*, 2009, **253**, 1649–1660.
40 D. Saggioro, M. P. Rigobello, L. Paloschi, A. Folda, S. A. Moggach, S. Parsons, L. Ronconi, D. Fregona and A. Bindoli, *Chem. Biol.*, 2007, **14**, 1128–1139.
41 Stoe & Cie. (2009). X-Area & X-RED32. Stoe & Cie GmbH, Darmstadt, Germany.
42 G. M. Sheldrick, *Acta Crystallogr., Sect. A: Found. Crystallogr.*, 2008, **64**, 112.

43 G. M. Sheldrick, *Acta Crystallogr., Sect. C: Struct. Chem.*, 2015, **71**, 3–8.
44 A. L. Spek, *Acta Crystallogr., Sect. D: Biol. Crystallogr.*, 2009, **65**, 148–155.
45 C. F. Macrae, I. J. Bruno, J. A. Chisholm, P. R. Edgington, P. M. Cabe, E. Pidcock, L. Rodriguez-Monge, R. Taylor, J. Streek and P. A. Wood, *J. Appl. Crystallogr.*, 2008, **41**, 466–470.
46 S. Zhu, W. Gorski, D. R. Powell and J. A. Walmsley, *Inorg. Chem.*, 2006, **45**, 2688–2694.
47 D. M. Motley, J. A. Walmsle, J. Zukerman-Schpector and E. R. T. Tiekink, *J. Chem. Crystallogr.*, 2009, **39**, 364–367.
48 A. Seliman, M. Altaf, A. Kawde, M. Wazeer and A. Isab, *J. Coord. Chem.*, 2014, **67**, 3431–3443.
49 N. Baig and A. Kawde, *Anal. Methods*, 2015, **7**, 9535–9541.

